

Magnetically amplified tunneling of the 3rd kind as a probe of minicharged particles

Babette Döbrich,^{1,2,*} Holger Gies,^{1,2} Norman Neitz,^{1,†} and Felix Karbstein^{1,2}

¹*Theoretisch-Physikalisches Institut, Friedrich-Schiller-Universität Jena, Max-Wien-Platz 1, D-07743 Jena, Germany*

²*Helmholtz-Institut Jena, Fröbelstieg 3, D-07743 Jena, Germany*

(Dated: June 2, 2022)

We show that magnetic fields significantly enhance a new tunneling mechanism in quantum-field theories with photons coupling to fermionic minicharged particles. We propose a dedicated laboratory experiment of the light-shining-through-walls type that can explore a parameter regime comparable to and even beyond the best model-independent cosmological bounds. With present-day technology, such an experiment is particularly sensitive to minicharged particles with masses in and below the meV regime as suggested by new physics extensions of the Standard Model.

PACS numbers: 14.80.-j, 12.20.Fv

Strong electromagnetic fields have recently become a powerful and topical laboratory probe of fundamental physics [1]. Together with precision optical probing, polarimetry experiments [2, 3] or experiments of the light-shining-through-walls (LSW) type [4–11] have provided the so far strongest laboratory – and thus model-independent – bounds on axion-like particles (ALPs) or minicharged particles (MCPs) [12]. Such hypothetical extremely weakly interacting particles occur in many new-physics models that are motivated by theoretical and observational puzzles in particle physics such as the strong-CP problem or dark-matter related anomalies. The particular power of laboratory experiments becomes obvious from the results of the ALPS experiment [11]: In a parameter window near the meV mass scale, ALPS provides for the most stringent bounds on hidden-sector photons (further U(1) gauge bosons). The maximum mass sensitivity scale of these experiments is typically set by the frequency scale of the optical probe lasers \sim eV, such that these experiments give access to a hypothetical new-physics regime of small masses but very weak couplings, complementary to collider experiments. The underlying mechanisms of induced polarimetric vacuum properties or photon-ALP conversion yield observables which at best saturate for small masses as the mass parameter effectively decouples in the small mass limit.

In the present work, we propose a search based on a new tunneling mechanism in quantum field theory [13]: here a photon can traverse an impenetrable barrier by virtue of virtual intermediate states that do not couple to the barrier. As it complements standard quantum mechanical tunneling and classical (tree-level) photon-ALP conversion, this phenomenon has been dubbed “tunneling of the 3rd kind”. It exploits the fluctuation-induced nonlocal properties of quantum field theory. In principle, such a phenomenon exists in the standard model with neutrinos as intermediate states, but the effective photon-neutrino couplings are extremely weak due to the Fermi constant [14]. For a search for new weakly interacting hypothetical particles, this is a benefit as any standard-model-physics background is strongly sup-

pressed [15] compared with the signatures considered in this work.

Whereas current laboratory bounds on minicharged particles are difficult to improve with tunneling of the 3rd kind at zero field, we demonstrate here that an external magnetic field can significantly amplify the tunneling probability for the case of minicharged fermions. The essence of the phenomenon lies in the existence of a near-zero mode in the Landau-type energy spectrum of fermionic minicharged fluctuations. As this zero mode is screened only by the MCP mass, the effect increases with a power-law dependence for decreasing MCP mass or increasing magnetic field and approaches a maximum at the pair-creation threshold.

Owing to this low-mass enhancement which is unprecedented so far in the context of strong-field physics, a dedicated laboratory experiment involving only present-day technology has the potential to explore a parameter space which so far had only been accessible with large-scale cosmological observations based on CMB data [16], see also [17]. Astrophysical considerations involving stellar energy loss arguments can even lead to stronger MCP constraints [18] but are somewhat model dependent [19, 20].

The experimental tunneling setting resembles standard LSW setups, as sketched in Fig. 1. A photon at frequency ω and momentum \mathbf{k} propagates orthogonally towards an opaque wall of thickness d . The system is put into a strong magnetic field $\mathbf{B} = B\hat{\mathbf{e}}_1$ at an angle $\theta = \sphericalangle(\mathbf{B}, \mathbf{k})$. A photon detector is placed behind the wall.

We analyze the new tunneling phenomenon within an (effective) microscopic quantum field theory with a QED-like Lagrangian, including a standard photon field A_μ , a Dirac spinor MCP ψ_ϵ (comments on scalar MCPs follow below), and an interaction of the form

$$\mathcal{L}_{\text{int}} = \epsilon e \bar{\psi}_\epsilon \gamma_\mu \psi_\epsilon A^\mu, \quad (1)$$

where ϵ parametrizes the potentially small coupling strength in units of the electron charge. The second unknown parameter of the theory is the potentially light MCP mass m . As we expect the MCPs to remain unobservable in direct measurements, we average over their

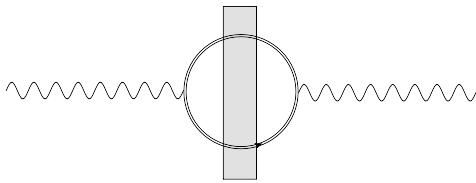


FIG. 1. Tunneling of a photon through a barrier mediated by a minicharged particle–antiparticle loop in a magnetic field. While this process is also possible in a zero-field situation, cf. [13], it is considerably enhanced in a strong magnetic field indicated by the solid double line of the minicharged intermediate states.

fluctuations. This leads to the effective Lagrangian for photon propagation in a strong electromagnetic field

$$\mathcal{L}[A] = -\frac{1}{4}F_{\mu\nu}F^{\mu\nu} - \frac{1}{2}\int_{x'} A_\mu(x)\Pi^{\mu\nu}(x, x'|B)A_\nu(x'), \quad (2)$$

where $\Pi^{\mu\nu}(x, x'|B)$ denotes the photon polarization tensor in the external field; here we have specialized to a magnetic field B which is assumed to be constant in all relevant spacetime regions, implying translational invariance for $\Pi^{\mu\nu}$ to one-loop order. Fluctuation-induced polarization effects of light propagating in a strong B field that follow from this Lagrangian have been discussed in [12, 21]. The associated equation of motion for the propagating photon in momentum space reads ($k^2 = \mathbf{k}^2 - \omega^2$)

$$(k^2 g^{\mu\nu} - k^\mu k^\nu + \Pi^{\mu\nu}(k|B)) A_\nu(k) = 0. \quad (3)$$

An important parameter in this context is provided by the strength of the magnetic field relative to the MCP mass scale. The most relevant regime for the present scenario is the strong-field domain, where $\epsilon\epsilon B/m^2 \gg 1$. A particular enhancement of the tunneling effect occurs for the Alfvén-like transversal mode with polarization in the (\mathbf{k}, \mathbf{B}) plane. For non-vanishing θ , this mode can be continuously related to one of the transversal modes at zero field. The second (magneto-acoustic) polarization mode receives no dominant magnetic enhancement; accordingly, the tunneling amplitude is not as strongly modified as for the Alfvén-like mode. Since photon propagation orthogonal to super-strong magnetic fields can be strongly damped [22–24], we consider a small angle between the direction of the magnetic field and the propagation direction, $\theta \gtrsim 0$. This is an important difference to standard LSW-type setups which typically employ $\theta = \pi/2$. The equation of motion for the Alfvén-like transversal mode A_T loses any nontrivial Lorentz index structure, $(k^2 + \Pi(k))A_T(k) = 0$, and the polarization tensor for this mode to leading order in the B field can be given as [25–27]

$$\Pi(k) = \frac{\epsilon^2 \alpha \epsilon \epsilon B}{2\pi} e^{-\frac{k_\perp^2}{2\epsilon\epsilon B}} \int_0^1 d\nu \frac{(1-\nu^2) k_\parallel^2}{m^2 - i\eta + \frac{1-\nu^2}{4} k_\parallel^2}, \quad (4)$$

where $k_\parallel = (\omega, k_1, 0, 0)$ and $k_\perp = (0, 0, k_2, k_3)$ denote the momentum components parallel and orthogonal to the B field, and the limit $\eta \rightarrow 0^+$ is implicitly understood. Subleading corrections to Eq. (4) are at most logarithmic in B . Retaining the full dependence on the photon momentum k_μ is essential here, since the computation of the outgoing amplitude behind the wall requires to take a Fourier transform back to position space. In the following, we assume reflecting boundary conditions at the wall for the incoming photons, in agreement with the use of a cavity to enhance the incoming photon flux. For the rear side, we assume absorbing boundary conditions. Other boundary conditions will lead to slightly different prefactors $\sim \mathcal{O}(1)$ in our final formulas. The probability for observing a photon at frequency ω behind the wall via tunneling of the 3rd kind arises from

$$P_{\gamma \rightarrow \gamma} = \left| \int_d^\infty dr' \frac{e^{-i\omega r'}}{2\omega} \int_{-\infty}^0 dr'' \Pi(r' - r'') \sin(\omega r'') \right|^2. \quad (5)$$

In principle $r' > d$ runs over all points on the optical axis between the rear side of the wall and the detector, whereas $r'' < 0$ extends over all points between the photon source and the front side of the wall. Hence, the r'' integral samples all nonlocal contributions arising from the incoming side and represents the source for the outgoing photons. The r' integral then coherently collects all outgoing photons convoluted with the outgoing Green's function. However, in Eq. (5) we have formally extended the respective integrations to $\pm\infty$. This is justified as $\Pi(r' - r'')$ receives its main contributions from relative distances $|r' - r''|$ of the order of the Compton wavelength $\sim 1/m$ of the MCPs, and falls off rapidly for $|r' - r''| \gg 1/m$. With respect to an actual experimental realization this implies that the magnetic field has to be sufficiently homogeneous only within a sphere of diameter $\gtrsim 1/m$ centered at the intersection of the optical axis with the wall. As we consider the wall as perfectly opaque, we neglect here potential couplings between the photons/MCPs and possible internal excitations of the wall in a magnetic field.

The transition probability can in general be evaluated numerically [28]; analytic expressions follow from Eq. (4) in various physically relevant limits. The full transition amplitude is discussed in more detail in [28]. In the following, we concentrate on a specific set of conservatively chosen parameters which can be experimentally realized with present-day technology. For the photon source and detection system, we consider state-of-the-art parameters as successfully installed and operated at ALPS [11]: The light of a frequency doubled standard laser light source, $\omega = 2.33$ eV ($\lambda = 532$ nm), is fed into an optical resonator cavity of length L to increase the light power available for MCP production. So far, ALPS has employed $L \simeq 4$ m, is currently upgrading to $L \simeq 10$ m, but aims at $L \sim 100$ m in its 2nd state of expansion, ALPS-II. Note that the di-

vergence $\Delta\theta$ of the laser beam in an optical cavity is given by $\Delta\theta = \sqrt{\lambda/(\pi L)}$, i.e., for $L = 10\text{m}$: $\Delta\theta = 0.0075^\circ$ ($L = 100\text{m}$: $\Delta\theta = 0.0024^\circ$).

The crucial difference to ALPS is the direction of the magnetic field, which in our scenario is at $\theta \gtrsim 0$, instead of $\theta = \pi/2$. As a suitable magnet we have identified a presently unused ZEUS compensation solenoid [29] available at DESY. It features a bore of 0.28m diameter and 1.20m length and provides a field strength of $B = 5\text{T}$. The field points along the bore, and is assumed to be adequately aligned on the solenoid's axis (accurate alignment studies of magnetic field lines relative to gravity have, e.g., been performed in [30] for a HERA dipole magnet). The field strength near the center of the solenoid is expected to be sufficiently homogeneous at least over a typical extent of the order of the bore's diameter. The wall is installed in the center of the bore and the back end of the cavity extends into the bore. The angle θ is adjusted by tilting the entire optics assembly relative to the solenoid's axis. Note that the detector position and its angular acceptance provides us with an additional handle to control θ . On the one hand, a larger field strength enhances the discovery potential. On the other hand, a sufficiently large spatial and temporal extent of the field is essential for the sensitivity towards low-mass particles. As discussed below Eq. (5), the length scale over which the field can be considered as approximately homogeneous should be comparable to or larger than the Compton wavelength of the minicharged particle. Thus, with the ZEUS compensation solenoid, access to MCP masses down to $m \gtrsim 7 \times 10^{-7}\text{eV}$ is granted.

Even though our tunneling phenomenon – contrary to LSW scenarios based on a tree-level process – intrinsically depends on the thickness of the wall, this dependence turns out to be negligible in the small-mass/strong-field limit which is of central interest here. We have checked that all our results presented below are valid up to at least $d = 1.8\text{cm}$ as used in [11].

In addition to the zero-field limit treated in [13], also the perturbative weak-field limit can be worked out analytically. However, even the leading-order correction to the transition amplitude $\sim (\epsilon e B/m^2)^2$ turns out to be quantitatively irrelevant in comparison to the zero-field effect for the present parameters. Moreover, the accessible minicharged parameter space where the perturbative expansion is valid is already ruled out by PVLAS data and cosmological bounds. It is the nonperturbative strong-field limit of the transition probability which gives access to a new region in the particle-physics parameter space. Here, a characteristic scale is provided by the condition for real pair creation

$$\omega \sin \theta \geq 2m. \quad (6)$$

In the no-pair-creation (npc), strong-field regime $\left\{ \frac{\epsilon e B}{m^2}, \frac{\epsilon e B}{\omega^2 \sin^2 \theta} \right\} \gg 1$, the transition probability is well

approximated by

$$P_{\gamma \rightarrow \gamma}^{(\text{strong, npc})} \simeq \frac{\epsilon^4 \alpha^2}{36\pi^2} \left(\frac{\epsilon e B}{m^2} \right)^2. \quad (7)$$

This astonishingly simple asymptotics can be understood in a physical picture associated with the quantum fluctuations: the typical length scale of the fluctuations is the Compton wavelength $\sim 1/m$. It dominates all other length scales $\sim d$ and $\sim 1/\omega$ here, rendering the transition probability d and ω independent in this regime. Equation (7) is also independent of θ and thus represents the maximally available transition probability in the limit $\theta \rightarrow 0$. However, for physically required finite values of θ , real pair creation eventually sets in if Eq. (6) is satisfied.

As real pairs are not expected to reconvert into photons, the photon-tunneling probability will drop beyond the pair creation (pc) threshold. In that strong-field regime with $\omega \sin \theta \gg 2m$, the transition probability for small angles θ becomes

$$P_{\gamma \rightarrow \gamma}^{(\text{strong, pc})} \simeq \frac{\epsilon^4 \alpha^2}{\pi^2} \frac{1}{\theta^8} \left(\frac{\epsilon e B}{\omega^2} \frac{4m^2}{\omega^2} \right)^2 \ln^2 \left(\frac{2m}{\omega} \right), \quad (8)$$

and hence depletes with smaller mass but enhances with smaller ω .

A prominent feature of Eqs. (7) and (8) is the quadratic dependence on the magnetic field, i.e., a linear dependence of the transition amplitude on the parameter $\epsilon e B$. This dependence leading to a small mass enhancement in Eq. (7) is a clear signature of IR dominance of the virtual fluctuations. This IR dominance can be understood in terms of the Landau level spectrum of virtual minicharged fluctuations in a magnetic field. The eigenvalues of the squared Dirac operator for the minicharged particles $\lambda_p = (p_\mu p^\mu) + m^2$ acquire the well-known Landau-level structure in a magnetic field,

$$\lambda_{p,j,\sigma} = -p_0^2 + p_\parallel^2 + \epsilon e B(2j + 1 + \sigma) + m^2. \quad (9)$$

where p_\parallel denotes the momentum component along the B field, j is the Landau-level index and $\sigma = \pm 1$ labels the spin eigenvalues with respect to the magnetic field. In the lowest Landau-level ($j = 0$) and for $\sigma = -1$, the eigenvalue reduces to a 1 + 1 dimensional zero-field spectrum. This dimensional reduction in quantum field theory goes along with an enhancement of long-range fluctuations. The linear B -field dependence of the amplitude then is dictated by the Landau-level measure in phase space. The long-range fluctuations can finally be screened only by the Compton wavelength or by real pair creation.

Our proposed setup in an LSW experiment is the first that suggests to exploit the characteristic near-zero mode of the spectrum of minicharged Dirac fermions. Other suggestions either work with photons near or on the light cone [31], with polarization properties [12] or with fluctuation-insensitive thermal production rates as in the

case of cosmological bounds [16]. These phenomena are less sensitive to minicharge masses and thus typically saturate in the low-mass limit.

An even stronger sensitivity arises near the pair creation threshold, where a resonance is encountered in the polarization tensor [32]. This resonance induces a singularity in the transition amplitude in the idealized limit of infinite coherent wave trains. If such resonances can be exploited also for realistic finite wave packets, an even larger parameter space could become accessible. In the present Letter we conservatively focus on the off-resonance regime, i.e., the parameter space that can be firmly excluded even if the encountered resonances would be smoothed out in an actual experimental realization.

The resulting observable in our setup is given by the outgoing photon rate on the rear side of the light-blocking wall,

$$n_{\text{out}} = \mathcal{N} n_{\text{in}} P_{\gamma \rightarrow \gamma}, \quad (10)$$

where n_{in} denotes the rate of incoming photons. The factor \mathcal{N} accounts for a possible regeneration cavity on the rear side of the wall. A feasibility study of this option even in the sub-quantum regime was recently successfully performed in a dedicated experiment [33]. In the absence of such a cavity, we have $\mathcal{N} = 1$.

As demonstrated at ALPS [11], present-day technology can achieve an incoming to outgoing photon ratio of $n_{\text{in}}/n_{\text{out}} = 10^{25}$, taking experimental issues such as the effective detector sensitivity, run time and the use of a front-side cavity into account. For the additional cavity on the regeneration side, a factor of $\mathcal{N} = 10^5$ appears realistic. A demanding issue with respect to an experimental implementation of our setting is the precise control of the angle θ , which preferably should be very small, $\theta \gtrsim 0$. In Fig. 2 we present results for $\theta \geq 0.001^\circ$. As discussed above, the uncertainty in the adjustment of θ is expected to be dominated by the beam divergence $\Delta\theta$. Notably, even with a divergence of $\Delta\theta = 0.0024^\circ$ exclusion bounds of the same quality as presented in Fig. 2 for $\theta = 0.001^\circ$ should become experimentally viable: Due to the fact that θ and $\Delta\theta > \theta$ are of comparable size, effectively both smaller and somewhat larger angles as $\theta = 0.001^\circ$ are sampled. Predictions for a concrete experimental set-up require, of course, a detailed modeling also including the profile of the cavity mode. However, we expect our present estimates to be affected only by prefactors of $\mathcal{O}(1)$.

In Fig. 2, we compare our resulting parameter space with current experimental exclusion limits [31] based on PVLAS polarization measurements [3] (purple/dotted line), and the best model-independent cosmological bounds [16] obtained from CMB data (blue/short-dashed line).

To summarize: even with the conservatively chosen parameters, we find that our magnetically amplified tunneling scenario can significantly enhance the discovery

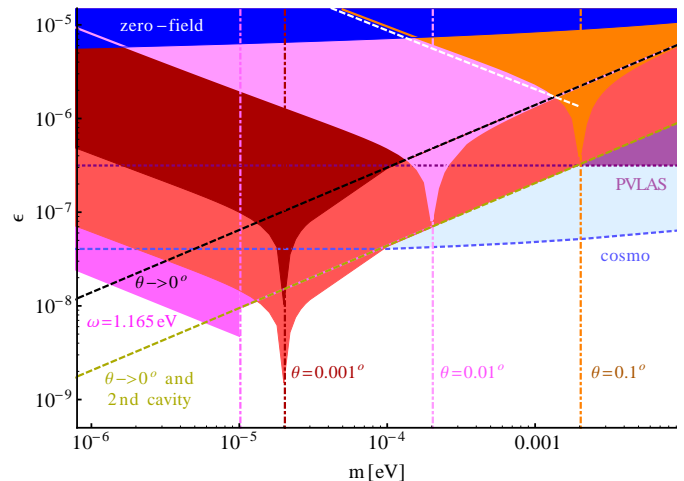


FIG. 2. Accessible minicharge parameter space based on tunneling via virtual minicharged particles employing ALPS parameters [11]. The transition at zero field gives access to the dark blue/dark shaded area, cf. [13]. The tunneling phenomenon is strongly amplified by a magnetic field (red-dish/gray shaded areas), and can be further enhanced by the use of a 2nd cavity on the rear side (lowermost light red/gray shaded area using $\mathcal{N} = 10^5$). The peak structures mark the resonance threshold (6) for various angles θ . As discussed in the main text, the steep cusps at the pair creation thresholds might be smoothed and less pronounced in an actual experimental realization. Our analytical estimate of Eq. (7) without (black) and with (yellow/gray) additional cavity are shown as dashed lines and agree with the numerically computed strong-field limit. The asymptotics (8) beyond the pair creation threshold is indicated for one particular case as white dashed line. A comparison is made with limits [31] derived from PVLAS polarization measurements [3] (purple/dotted line), and the best model-independent cosmological bounds [16] (blue/short-dashed line). Our setup has the potential to outmatch these bounds with a regeneration cavity below $m \lesssim 9 \times 10^{-5} \text{eV}$ with/without a fundamental mode laser at $\omega = 1.165 \text{eV}$ (asymptotics indicated by the lower-left magenta area).

potential for minicharged particles in an LSW experiment. This setup can improve PVLAS polarization data for minicharged particles below $m \lesssim 2 \times 10^{-4} \text{eV}$. Employing a cavity on the regeneration side with/without a laser in the fundamental mode with $\lambda = 1064 \text{nm}$ ($\omega = 1.165 \text{eV}$), these values can even be improved beyond PVLAS bounds for $m \lesssim 2 \times 10^{-3} \text{eV}$ and cosmological bounds below $m \lesssim 9 \times 10^{-5} \text{eV}$.

As this mechanism of magnetic amplification is only active for Dirac fermionic fluctuations due to the underlying Landau-level structure, our proposal can decisively distinguish between minicharged scalars or fermions.

Finally, it appears worthwhile to consider similar ideas also on terrestrial or astrophysical scales, as magnetic fields of larger extent might give access to even further regions of the minicharged particle parameter space.

BD, HG and NN acknowledge support by the DFG

under grants SFB-TR18 and GI 328/5-2 (Heisenberg program) as well as GRK-1523. We thank J. Jaeckel, A. Lindner and D. Trines for interesting discussions and helpful correspondence.

* Now at DESY, Notkestraße 85, D-22607 Hamburg, Germany.

† Now at Max-Planck-Institut für Kernphysik, Saupfercheckweg 1, D-69117 Heidelberg, Germany.

- [1] H. Gies, *J. Phys. A* **41**, 164039 (2008); J. Jaeckel and A. Ringwald, *Ann. Rev. Nucl. Part. Sci.* **60**, 405 (2010); J. Redondo and A. Ringwald, *Contemp. Phys.* **52**, 211 (2011).
- [2] R. Cameron *et al.*, *Phys. Rev. D* **47**, 3707 (1993).
- [3] E. Zavattini *et al.* [PVLAS Collaboration], *Phys. Rev. D* **77**, 032006 (2008).
- [4] A. A. Anselm, *Yad. Fiz.* **42**, 1480 (1985); P. Sikivie, *Phys. Rev. Lett.* **51** (1983) 1415 [Erratum-ibid. **52** (1984) 695]; K. Van Bibber *et al.* *Phys. Rev. Lett.* **59**, 759 (1987).
- [5] A. S. Chou *et al.* [GammeV (T-969) Collaboration], *Phys. Rev. Lett.* **100**, 080402 (2008).
- [6] C. Robilliard *et al.*, *Phys. Rev. Lett.* **99**, 190403 (2007).
- [7] M. Fouche *et al.*, *Phys. Rev. D* **78**, 032013 (2008).
- [8] A. Afanasev *et al.*, *Phys. Rev. Lett.* **101**, 120401 (2008).
- [9] P. Pognat *et al.* [OSQAR Collaboration], *Phys. Rev. D* **78**, 092003 (2008).
- [10] R. Battesti *et al.*, *Phys. Rev. Lett.* **105**, 250405 (2010).
- [11] K. Ehret *et al.*, *Phys. Lett. B* **689**, 149 (2010).
- [12] H. Gies, J. Jaeckel and A. Ringwald, *Phys. Rev. Lett.* **97**, 140402 (2006).
- [13] H. Gies and J. Jaeckel, *JHEP* **0908**, 063 (2009).
- [14] H. Gies and R. Shaisultanov, *Phys. Rev. D* **62**, 073003 (2000).
- [15] M. Ahlers, J. Jaeckel, J. Redondo and A. Ringwald, *Phys. Rev. D* **78**, 075005 (2008).
- [16] A. Melchiorri, A. Polosa and A. Strumia, *Phys. Lett. B* **650**, 416 (2007).
- [17] M. Ahlers, *Phys. Rev. D* **80**, 023513 (2009); C. Burrage, J. Jaeckel, J. Redondo and A. Ringwald, *JCAP* **0911**, 002 (2009).
- [18] S. Davidson, S. Hannestad and G. Raffelt, *JHEP* **0005**, 003 (2000).
- [19] E. Masso and J. Redondo, *Phys. Rev. Lett.* **97**, 151802 (2006).
- [20] J. Jaeckel, E. Masso, J. Redondo, A. Ringwald and F. Takahashi, *Phys. Rev. D* **75**, 013004 (2007).
- [21] M. Ahlers, H. Gies, J. Jaeckel and A. Ringwald, *Phys. Rev. D* **75**, 035011 (2007).
- [22] D. B. Melrose and R. J. Stoneham, *Nuovo Cim. A* **32**, 435 (1976).
- [23] W. Dittrich and H. Gies, *Springer Tracts Mod. Phys.* **166**, 1 (2000).
- [24] A. E. Shabad, *Annals Phys.* **90**, 166 (1975).
- [25] B. Döbrich and F. Karbstein, in preparation (2012).
- [26] F. Karbstein, L. Roessler, B. Döbrich and H. Gies, *Int. J. Mod. Phys. Conf. Ser.* **14**, 403 (2012).
- [27] A. E. Shabad, arXiv:hep-th/0307214.
- [28] B. Döbrich, H. Gies, N. Neitz and F. Karbstein, arXiv:1203.4986 [hep-ph].
- [29] O. Dormicchi, R. Penco, S. Parodi, P. Valente, A. Bonito Oliva, G. Gaggero, M. Losasso and G. Masullo *et al.*, *IEEE Trans. Magnetics* **27**, 1958 (1991).
- [30] R. Meinke, *IEEE Trans. Magnetics* **27**, 1728 (1991).
- [31] M. Ahlers, H. Gies, J. Jaeckel, J. Redondo and A. Ringwald, *Phys. Rev. D* **77**, 095001 (2008).
- [32] A. E. Shabad, *Lett. Nuovo Cim.* **3S2**, 457 (1972); N. S. Witte, *J. Phys.A: Math.Gen.* **23**, 5257 (1990).
- [33] J. G. Hartnett, J. Jaeckel, R. G. Povey and M. E. Tobar, *Phys. Lett. B* **698**, 346 (2011).